made as above, and the values for δ and K_d were comparable with the two approaches.
13. P. H. Backx, E. Marban, D. T. Yue, *Biophys. J.* **57**, 298a (1990); S. Visentin *et al.*, *Pfluegers Arch.* **417**, 213 (1990).
14. The K_d's for Cd^{2+} blockage at 0 mV determined from plots of the open probability at various voltages were 6.8 mM for μI (r = 0.995) and 100 μM for native cardiac channels (r = 0.985).
15. In similar experiments, Zn^{2+} blockage of cardiac and μI skeletal muscle Na^+ channels was examined. The K_d's for Zn^{2+} were similar to those measured for Cd^{2+}, and estimates for the electrical distance of the binding site in the membrane field were virtually identical.
16. R. B. Rogart *et al.*, *Proc. Natl. Acad. Sci. U.S.A.* **86**, 8170 (1989).
17. A. E. Martell and R. M. Smith, *Critical Stability Constants: Amino Acids* (Plenum, New York, 1989), vol. 1, p. 47.
18. J. M. Berg, *Annu. Rev. Biophys. Biophys. Chem.* **19**, 405 (1990).
19. The 1.9-kb Bam HI–Sph I fragment from the μ1-2 cDNA (*8*) was subcloned into pGEM-11Zf+ for mutagenesis [T. A. Kunkel, *Proc. Natl. Acad. Sci. U.S.A.* **82**, 488 (1985)]. The entire fragment was sequenced by the dideoxy chain termination method (Sequenase, U.S. Biochemical) [F. Sanger *et al.*, *Proc. Natl. Acad. Sci. U.S.A.* **74**, 5463 (1977)]. In vitro RNA transcription and oocyte injection were done as described (*9*).
20. M. Baer *et al.*, *Nature* **263**, 344 (1976); C. J. Cohen *et al.*, *J. Gen. Physiol.* **78**, 383 (1981); P. M. Vassilev *et al.*, *Am. J. Physiol.* **251**, H475 (1986); B. Hille, *Biophys. J.* **15**, 615 (1975); *J. Gen. Physiol.* **66**, 535 (1975).
21. Oocytes injected with RNA that encoded the wild-type μI Na^+ channel α subunit and the Y401C mutation were voltage-clamped with a two-microelectrode amplifier. Currents were recorded in 96 mM NaCl, 2 mM KCl, 0.5 mM $CaCl_2$, and 5 mM Hepes (pH 7.5). TTX was added to the bath at concentrations from 1 nM to 1 μM (wild type) and 100 nM to 50 μM (Y401C). Peak currents were measured at −10 mV from a holding potential of −120 mV and were normalized to the current in the absence of toxin. The data represent at least three determinations at each concentration from 20 (wild type) and 13 (Y401C) oocytes. The wild-type K_d was determined by a least-squares fit of the data to a logistic function; a similar fit to the Y401C mutant was not possible because of the insensitivity of the variant to TTX (Fig. 2B).
22. The mutant Y401C actually is less sensitive to TTX (K_d > 50 μM) and more sensitive to blockage by Cd^{2+} (K_d at 0 mV = 29 μM; r = .981; n = 6) than native cardiac channels. The differences presumably arise from other residues that differ between the two channels.
23. J. Satin *et al.*, *Science* **256**, 1202 (1992).
24. M. F. Sheets and D. A. Hanck, *J. Physiol.* (*London*), in press.
25. D. T. Yue and E. Marban, *J. Gen. Physiol.* **95**, 911 (1990).
26. We thank G. Breitwieser and G. Yellen for helpful comments on the manuscript and K. Kluge and R. Xu for technical assistance. Supported by the Medical Research Council of Canada (P.H.B.), Established Investigator of the American Heart Association (D.T.Y.), NIH grant K11 HL02639 (J.H.L.), NIH grant RO1 HL36957 (E.M.), and NIH grant K08 HL2421 (G.F.T.).

27 February 1992; accepted 8 May 1992

Block of Ca^{2+} Wave and Ca^{2+} Oscillation by Antibody to the Inositol 1,4,5-Trisphosphate Receptor in Fertilized Hamster Eggs

Shun-ichi Miyazaki,* Michisuke Yuzaki, Ken Nakada, Hideki Shirakawa, Setsuko Nakanishi, Shinji Nakade, Katsuhiko Mikoshiba

The concentration of cytoplasmic free calcium (Ca^{2+}) increases in various stimulated cells in a wave (Ca^{2+} wave) and in periodic transients (Ca^{2+} oscillations). These phenomena are explained by inositol 1,4,5-trisphosphate (IP_3)–induced Ca^{2+} release (IICR) and Ca^{2+}-induced Ca^{2+} release (CICR) from separate intracellular stores, but decisive evidence is lacking. A monoclonal antibody to the IP_3 receptor inhibited both IICR and CICR upon injection of IP_3 and Ca^{2+} into hamster eggs, respectively. The antibody completely blocked sperm-induced Ca^{2+} waves and Ca^{2+} oscillations. The results indicate that Ca^2 release in fertilized hamster eggs is mediated solely by the IP_3 receptor, and Ca^{2+}-sensitized IICR, but not CICR, generates Ca^{2+} waves and Ca^{2+} oscillations.

A dramatic, transient increase in the intracellular calcium (Ca^{2+}) concentration ($[Ca^{2+}]_i$) occurs at fertilization in all eggs investigated so far, observed as a "Ca^{2+} wave" across the egg (*1*). In many species the Ca^{2+} transient is due to release of intracellular Ca^{2+} (*1*) and is required for exocytosis of cortical granules to prevent polyspermy (*1*) and for cell cycle progression (*2*). Fertilized hamster eggs exhibit repetitive Ca^{2+} transients as well as the Ca^{2+} wave in each response (*3*). Ca^{2+} waves and Ca^{2+} oscillations commonly occur in various somatic cells in response to neurotransmitters, hormones, and growth factors (*4*, *5*). These agents stimulate polyphosphoinositide turnover, which leads to IICR (*4*). IICR is suggested to occur in fertilized eggs of the sea urchin (*2*), frog (*6*), and hamster (*7*). On the other hand, IP_3-independent Ca^{2+} release, such as CICR, has also been detected in sea urchin eggs (*8*, *9*) and other cells (*4*). However, it has been difficult to obtain direct evidence for operation of IICR, or of CICR after eliminating IICR, in functioning cells under physiological conditions, because no specific blockers of IICR were available.

IICR and CICR are mediated by the IP_3 receptor (*10*, *11*) and ryanodine receptor (*12*), respectively. The IP_3 receptor has been purified from rat (*10*) and mouse (*11*) cerebella, and its primary structure was determined by cDNA cloning (*13*, *14*). Three monoclonal antibodies (MAbs) to the mouse IP_3 receptor have been obtained (*11*, *13*). The 18A10 MAb, which recognizes an epitope close to the proposed Ca^{2+} channel region in the COOH-terminus of the receptor protein (*13*), inhibits IICR in mouse cerebellar microsomes (*15*), whereas 4C11 and 10A6, which recognize the NH_2-terminal and middle regions, respectively (*13*), block neither IP_3 binding nor Ca^{2+} release in microsomes (*15*). We investigated whether 18A10 could block Ca^{2+} release induced by injection of IP_3 or by sperm in hamster eggs.

In hamster eggs, 18A10 stained the cortical area and inner cytoplasm in a roughly reticular pattern (Fig. 1A) (*11*), consistent with the distribution of smooth endoplasmic reticula (*16*). Eggs were also stained by 4C11 but not by 10A6. We ascertained the specificity of the MAbs by immunostaining of blotted proteins from hamster eggs (Fig. 1B) (*11*). Both 18A10 and 4C11 stained a single 250-kD protein corresponding to the mouse IP_3 receptor (*11*). The 10A6 MAb stained the 250-kD band from eggs faintly, although it reacted strongly with a 250-kD protein from cerebella and ovaries after ovulation of mature eggs. In this report, 4C11 and 10A6 served as controls.

Each MAb was injected into eggs through micropipettes by air pressure, together with the Ca^{2+}-sensitive dye fura 2. Measurement of fluorescence of fura 2 enabled estimation of the injected volume of MAb and measurement of $[Ca^{2+}]_i$ with an image processor (*17*). IP_3 was injected at the margin of the egg 1 to 2 hours later with negative current pulses (Fig. 2), which allowed repeated application of IP_3 in the same egg. The relative amount of IP_3 administered is represented by the magnitude (nA × s) of the square current pulse. The spatial distribution of increases in $[Ca^{2+}]_i$ was analyzed at three areas (Fig. 2).

S-i. Miyazaki, K. Nakada, H. Shirakawa, Department of Physiology, Tokyo Women's Medical College, 8-1 Kawada-cho, Shinjuku-ku, Tokyo 162, Japan.
M. Yuzaki, Department of Biochemistry, Jichi Medical School, Tochigi-ken 329-04, Japan.
S. Nakanishi and S. Nakade, Division of Regulation of Macromolecular Function, Institute for Protein Research, Osaka University, Suita 565, Japan.
K. Mikoshiba, Department of Molecular Neurobiology, Institute of Medical Science, University of Tokyo, Minato-ku, Tokyo 108, Japan.

*To whom correspondence should be addressed.

Injection of IP_3 (0.9 nA × 1 s-pulse) caused a small rise in $[Ca^{2+}]_i$ with a peak of 100 to 200 nM that was the highest at the injection site (Fig. 2A); locally released Ca^{2+} ions diffused toward the opposite side. With a 1-nA pulse, the peak $[Ca^{2+}]_i$ reached 500 to 550 nM in the whole egg, and a nonlinear regenerative response was induced. The $[Ca^{2+}]_i$ increased ~2 s later at the side of the egg opposite the injection site, whereas peak $[Ca^{2+}]_i$ was nearly the same throughout the egg (Fig. 2A), indicating that the increase in $[Ca^{2+}]_i$ is due to propagated Ca^{2+} release rather than to diffusion of Ca^{2+}. The regenerative response was also induced by IP_3 in eggs injected with 4C11 (Fig. 3A) or 10A6.

The 18A10 MAb inhibits IICR (Fig. 2B). The increase in $[Ca^{2+}]_i$ in eggs treated with 18A10 was graded in response to increasing doses of IP_3. The $[Ca^{2+}]_i$ was lower at the opposite side, even if $[Ca^{2+}]_i$ at the injection site reached 350 to 450 nM for pulses up to 10 nA (Fig. 2B); propagated Ca^{2+} release was inhibited by 18A10 (Fig. 3B, 5 nA × 1.5-s pulse). Thus, IICR is involved in propagation of Ca^{2+} release, not only as the initial trigger at the injection site. With larger doses of IP_3, the increase in $[Ca^{2+}]_i$ was not restricted to a local area, probably because the injected IP_3 spread over a wider area.

The inhibition of peak $[Ca^{2+}]_i$ was dependent on the intracellular 18A10 concentration ($[18A10]_i$) (Fig. 2C); the inhibition curve shifted to the right, and its slope was reduced with an increasing $[18A10]_i$. The regenerative Ca^{2+} release induced by IP_3 (1 nA × 1-s pulse) was completely blocked at an $[18A10]_i$ of 30 μg/ml, whereas it was not suppressed by 4C11 (420 μg/ml) or 10A6 (540 μg/ml) (Fig. 2C). The inhibitory effect of 18A10 was compensated by increasing doses of IP_3, but the response to a 20 nA × 2-s pulse, which was nearly maximal, was substantially suppressed by 18A10 in a dose-dependent manner (Fig. 2C), suggesting that the mode of inhibition is noncompetitive. Binding assays in microsomes showed that 18A10 does not inhibit IP_3-receptor binding (*15*). The MAb reacts with the 12 amino acid residues near the Ca^{2+} channel region (*15*). Binding of 18A10 may cause partial occlusion or conformational change in the channel.

In hamster eggs a single sperm induces repetitive Ca^{2+} transients over a period of 1 hour (*3*). The initial three to four responses occur at short intervals (Fig. 4A), starting when flagellar motion of the attached sperm stops, probably on sperm-egg fusion (*3*). Later responses occur at intervals of 2 to 3 min, which are superimposed on a slightly elevated basal $[Ca^{2+}]_i$ (Fig. 4A). Each Ca^{2+} transient is preceded by a slower and

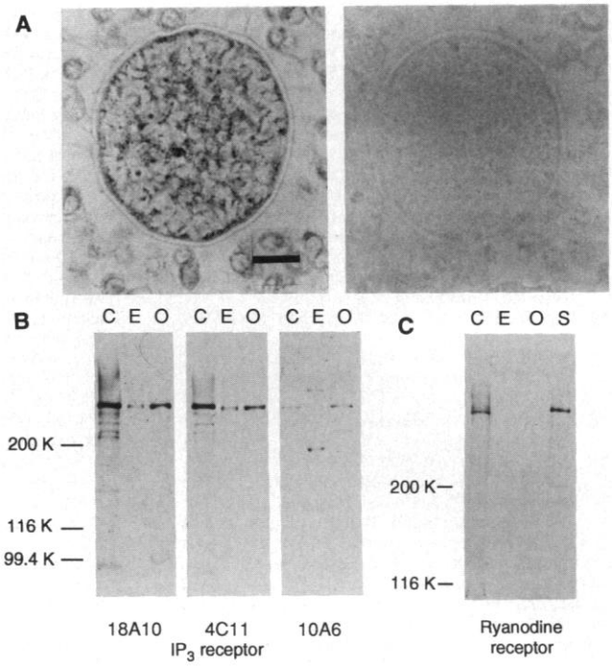

Fig. 1. Reactivity of MAbs to the mouse IP_3 receptor and polyclonal antibody to the rabbit ryanodine receptor with proteins from hamster eggs. (**A**) Immunohistochemical staining with 18A10 (100 μg/ml) (left) and without 18A10 (right). Scale bar is 15 μm. (**B**) Immunoblots of total protein from 80 mature eggs (E) freed from the zona pellucida (estimated as 0.6 μg of protein) and proteins from microsomal fraction of hamster cerebellum (1 μg) (C) and ovary (O) after ovulation of mature eggs (4 μg), probed with three MAbs (5 μg/ml) (*11*). (**C**) Blots probed with polyclonal antibody to peptide of the ryanodine receptor (Asn 4929–Arg 4949 of cardiac muscle type, identical to the corresponding region of skeletal muscle type, 1 μg/ml). C, hamster cerebellum (10 μg of protein); E, 80 eggs; O, ovary (10 μg); S, skeletal muscle (2 μg).

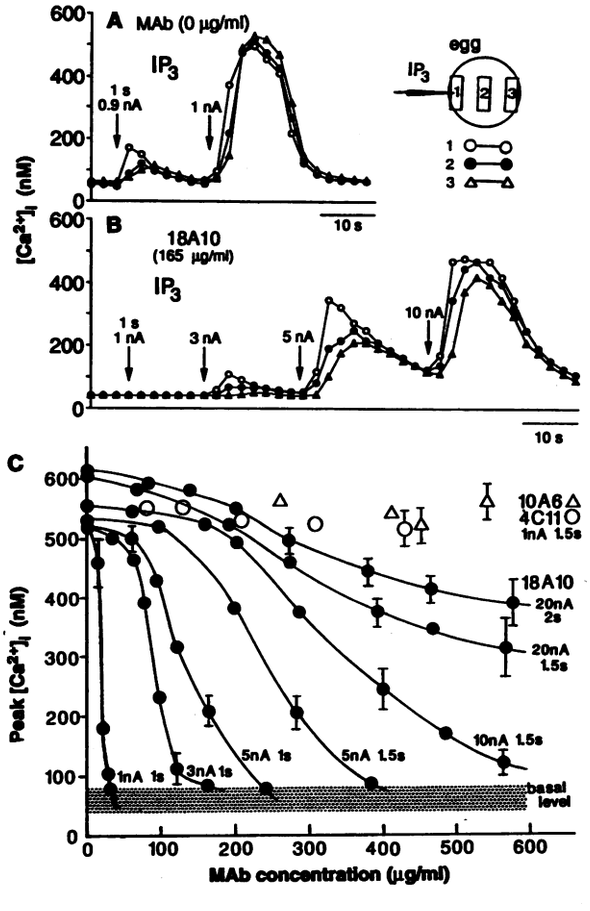

Fig. 2. Inhibition of IICR by 18A10. $[Ca^{2+}]_i$ rise upon IP_3 injection (arrows) without MAb (**A**) and with 18A10 (**B**). Inset shows position of pipette and areas in which $[Ca^{2+}]_i$ was measured. (**C**) Relation between $[MAb]_i$ and peak $[Ca^{2+}]_i$ (averaged in the whole egg) with various pulses indicated for IP_3 injection, which was performed once or twice in an egg in most cases (three to four times in a few cases). Repetitive injections of IP_3 were performed when the previous response was small enough not to affect the next Ca^{2+} release. Because the volume injected was not precisely controlled at a given value, the values of $[MAb]_i$ within the range of 15 μg/ml are presented by the mean value. Points with vertical bars represent mean ± SD of three to five eggs (SD is omitted in the points on the ordinate). Each point without a bar represents the value from one egg. Values obtained from 107 IP_3 injections in 75 eggs fall on the points and bars. The maximum $[MAb]_i$ obtainable with the present method was about 600 μg/ml. All experiments were done at 30° to 32°C.

smaller increase in $[Ca^{2+}]_i$, and their transition occurs at 150 to 170 nM. Responses in the presence of 4C11 (Fig. 4B) or 10A6 were normal. The Ca^{2+} wave started from the sperm attachment site (Fig. 3C), and it could be recognized (Fig. 4B, first two responses) by the slower increases in $[Ca^{2+}]_i$ with identical peak concentrations at the three areas monitored.

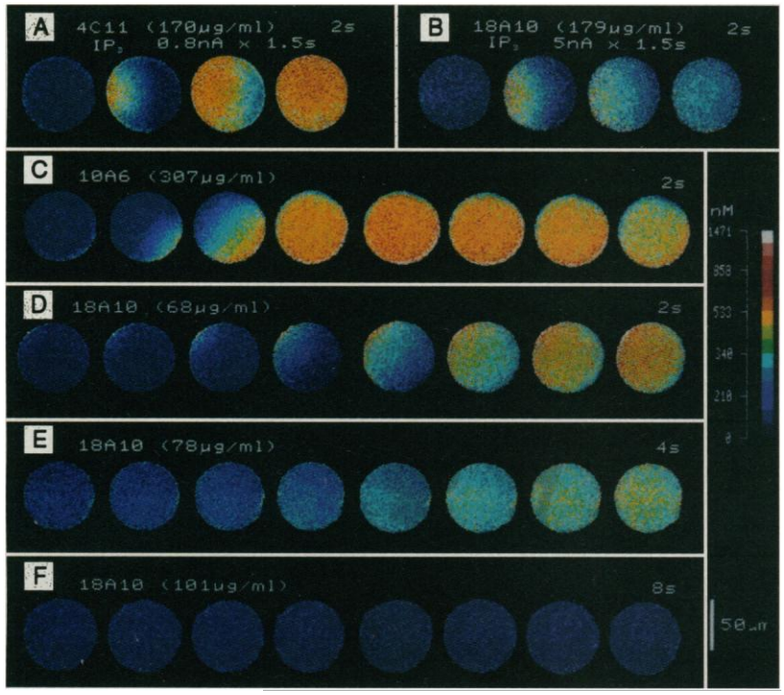

Fig. 3. Pseudo-colored Ca^{2+} images from the rising phase of Ca^{2+} transients. (**A** and **B**) IICR in the presence of 4C11 or 18A10 with injection pulse of IP_3 indicated. (**C** to **F**) The first rise in $[Ca^{2+}]_i$ in fertilized eggs treated with MAb. Sperm were drawn on the computer display. Each image is a combination of F_{340}/F_{360} images (*17*) accumulated during 0.5-s intervals every 2 s in (A) to (D), 4 s in (E), and 8 s in (F). The egg in (E) is the same egg as in Fig. 4C, broken line.

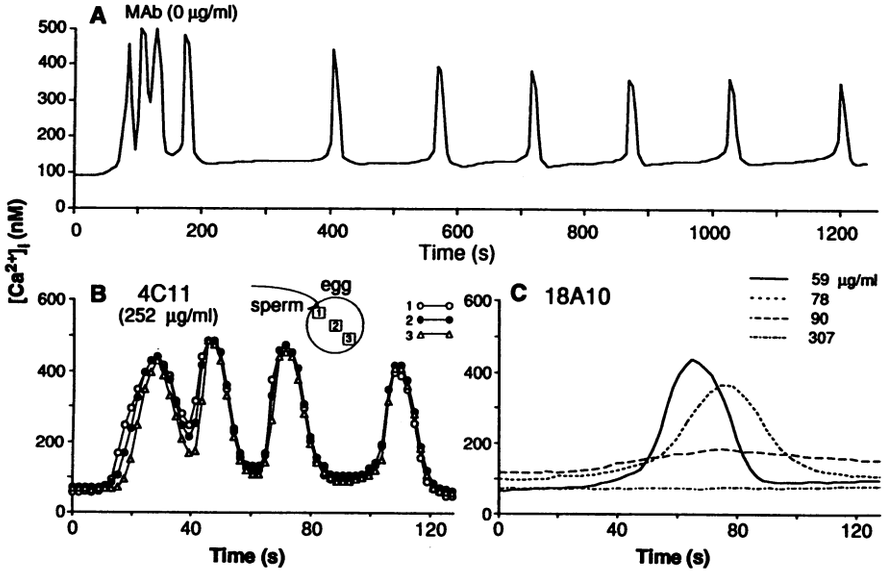

Fig. 4. Inhibition of sperm-induced Ca^{2+} transients by 18A10. (**A**) Ca^{2+} transients (averaged in the whole egg) in a fertilized egg without MAb. Initial responses induced by a sperm in a 4C11-treated egg (**B**) and four eggs injected with 18A10 at various concentrations (**C**). Inset shows areas of measurement. Sperm were applied 1 to 2 hours after injection of MAb. Recording in the dark field was started (zero time) immediately after the attachment of the first sperm to the egg surface. Fusion of the single sperm with the egg was identified after the recording by stopped flagellar motion.

The number of initial Ca^{2+} transients reduced to one or two in most cases by 18A10 (50 to 100 μg/ml), and the increase in $[Ca^{2+}]_i$ was smaller and slower as $[18A10]_i$ increased (Fig. 4C). Propagation time of the Ca^{2+} wave over the entire egg was delayed by 5 to 10 s by 18A10 (Fig. 3, D and E). Ca^{2+} transients by a single sperm were completely blocked by $[18A10]_i$ greater than 100 μg/ml (n = 30) (Fig. 4C). No local rise in $[Ca^{2+}]_i$ was detected even at the sperm attachment site (Fig. 3F). Thus, IICR is the primary mechanism for the initiation of sperm-induced Ca^{2+} transients and is responsible for the propagating rise in $[Ca^{2+}]_i$.

Because eggs were freed from the surrounding zona pellucida, polyspermy block is absent, even if exocytosis of cortical granules is induced by increased $[Ca^{2+}]_i$. Additional sperm that fuse to the egg tend to cause more frequent Ca^{2+} oscillations (*3*). The number of Ca^{2+} transients in 10 min was 5.8 ± 0.8 (n = 9) in control eggs, 3.8 ± 1.2 (n = 4) at an $[18A10]_i$ of 50 to 60 μg/ml and 1.6 ± 0.8 (n = 7) at 80 to 90 μg/ml. No response was induced even by several sperm when $[18A10]_i$ was more than 100 μg/ml (n = 14). Thus, 18A10 suppressed the frequency of sperm-induced Ca^{2+} oscillations in a dose-dependent manner, comparable to the inhibition of IICR for pulses a little smaller than 3 nA × 1 s (Fig. 2C) (about threefold greater than the threshold pulse for inducing regenerative Ca^{2+} release).

Both IP_3-dependent and IP_3-independent Ca^{2+} release from separate stores has been shown in sea urchin eggs and a Ca^{2+} transient is induced by sperm even in eggs injected with heparin, a blocker of IICR (*8*). Ryanodine receptor–mediated CICR has been detected in sea urchin egg homogenates (9). In hamster eggs, injection of Ca^{2+} causes a hyperpolarizing response (HR) in membrane potential due to a Ca^{2+}-activated K^+ current, and increasing doses of Ca^{2+} induce a regenerative HR in Ca^{2+}-free medium (*18*). Correspondingly, a regenerative and propagating rise in $[Ca^{2+}]_i$ was evoked when $[Ca^{2+}]_i$ was raised to 250 to 350 nM by injected Ca^{2+} (Fig. 5A), similar to IP_3-induced responses. The same or even greater doses of Ca^{2+} failed to induce the next regenerative response during 1 to 2 min after the previous response. These results suggest CICR and a subsequent depletion of Ca^{2+} stores.

This apparent CICR was inhibited by 18A10 (Fig. 5B); only graded rises in $[Ca^{2+}]_i$ with the spatial gradient from the injection site down to the opposite side were produced by injected Ca^{2+} and its diffusion, up to 900 nM at the injection site. On the other hand, caffeine (1 to 5 mM in the egg) neither induced Ca^{2+} release nor lowered

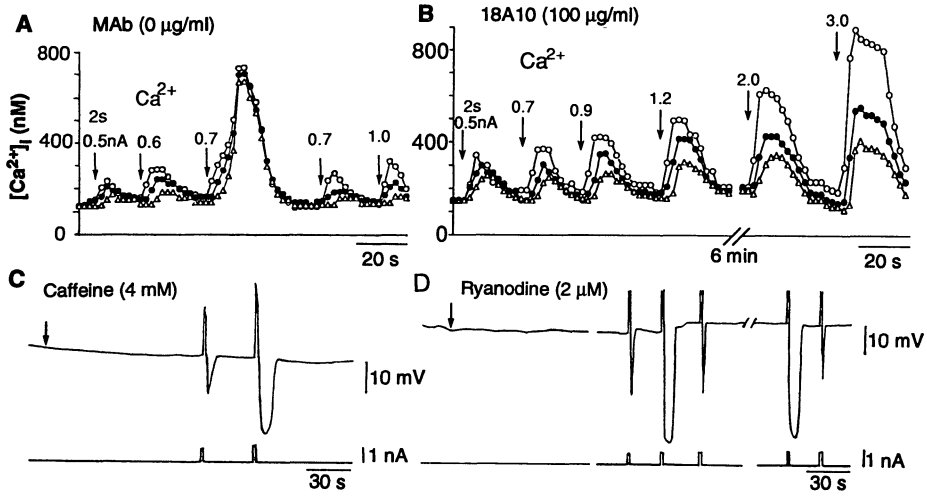

Fig. 5. (**A** and **B**) Increase in $[Ca^{2+}]_i$ upon injection of Ca^{2+} in the absence and presence of 18A10. Positive current pulses were applied to the injection pipette filled with 20 mM $CaCl_2$. See inset of Fig. 2A for symbols. (**C**) Injection of caffeine (arrow; 4 mM in the egg) without causing HR in membrane potential. A regenerative HR was normally induced by Ca^{2+} injection with 1 nA × 2-s pulse (bottom trace), without sensitization by caffeine. Fura 2 imaging was not used to watch caffeine injection by pressure in the bright field. (**D**) Injection of ryanodine (arrow) without any response, and subsequent Ca^{2+} injection inducing regenerative HRs.

the threshold of Ca^{2+} injection to induce the regenerative response (Fig. 5C), and ryanodine (0.5 to 25 μM in the egg) neither induced Ca^{2+} release nor blocked the apparent CICR (Fig. 5D), unlike ryanodine receptor–mediated Ca^{2+} release in smooth muscles (*19*). The ryanodine receptor was not detected in hamster eggs by immunoblot analysis with an antibody to the rabbit ryanodine receptor, whereas a protein of about 400 kD from skeletal muscles and cerebellum was stained (Fig. 1C), comparable to the receptor from rabbit muscle (*12*). The possibility of 18A10 cross-reacting with the ryanodine receptor or putative receptors such as sulfhydryl reagent-reactive 106-kD Ca^{2+} release channel (*20*) is excluded by immunoblot showing a single band at the 250-kD IP_3 receptor (Fig. 1B). All these findings indicate that the apparent CICR is mediated by the IP_3 receptor. This is a striking difference from CICR in sea urchin eggs (*8*, *9*).

We revealed that 18A10 blocks apparent CICR as well as IICR and that IP_3 receptor–mediated Ca^{2+} release is the primary and essential mechanism for Ca^{2+} waves and Ca^{2+} oscillations in fertilized hamster eggs. This is the first successful application of the function-blocking antibody to the IP_3 receptor. This MAb will be a useful tool in dissecting the molecular mechanisms of Ca^{2+} signals in other cell types.

Generation of Ca^{2+} waves requires a regenerative or autocatalytic process of Ca^{2+} release. Especially in hamster eggs, positive feedback between Ca^{2+} and IICR is necessary because Ca^{2+} release is mediated solely by the IP_3 receptor. A candidate for the positive feedback loop is recycle between Ca^{2+} release induced by IP_3 and Ca^{2+}-dependent production of IP_3 (*21*, *22*); a local rise in $[Ca^{2+}]_i$ by IICR activates phospholipase C in the plasma membrane, which leads to IICR in neighboring Ca^{2+} pools in the cortical area. Another possible mechanism is the sensitization of IICR by elevated $[Ca^{2+}]_i$. IICR in skinned smooth muscle fibers is enhanced by increasing $[Ca^{2+}]_i$ between 0 and 300 nM (*23*), and the maximum probability of opening of IP_3-gated Ca^{2+} channels in lipid bilayers occurs at $[Ca^{2+}]$ of 200 nM (*24*). Correspondingly, in hamster eggs, IP_3- or Ca^{2+}-induced regenerative responses arise from the apparent threshold of $[Ca^{2+}]_i$ between 200 and 300 nM (Figs. 2A and 5A), and sperm-induced Ca^{2+} transients arise from about 160 nM (Fig. 4, A and B). Increases in $[Ca^{2+}]_i$ at fertilization were detected in the deep cytoplasm, not only in the cortical area (*25*). The distribution of the 18A10-stained area (Fig. 1A) is consistent with this finding. Thus, it is reasonable to consider that Ca^{2+} ions mobilized from IP_3-sensitive pools at the sperm-attachment site sensitize neighboring, deeper pools to release Ca^{2+} at lower $[IP_3]_i$. This process can occur in succession, resulting in a Ca^{2+} wave.

To explain Ca^{2+} oscillations, several models have been proposed. One of the leading models is a two-pool model, which postulates that the stimulus of IP_3 is persistent and that IICR from IP_3-sensitive Ca^{2+} pools constantly provides Ca^{2+} which fills previously emptied IP_3-insensitive pools and leads to repeated CICR (*4*). Another model is based on a single (IP_3-sensitive) pool and postulates oscillation in $[IP_3]_i$ through a feedback loop (*22*, *26*). In fertilized hamster eggs, evidence suggests persistent stimulus of IP_3 (*27*), and this study showed that Ca^{2+} oscillations are generated only by IICR. We thus present here a different single-pool model to operate in an intact cell system, based on Ca^{2+}-sensitized IICR instead of CICR and the supply of Ca^{2+} from external medium. Ca^{2+} oscillations depend on the sensitivity of IP_3 receptors and basal $[Ca^{2+}]_i$ (*28*). The frequency and magnitude are suppressed by 18A10 (Fig. 4), which reduces overall receptor sensitivity (Fig. 2). The slight elevation of basal $[Ca^{2+}]_i$ produced by sperm (Fig. 4A) can cause sensitization of IICR and promote refilling of IP_3-sensitive pools and thereby maintain Ca^{2+} oscillations at low $[IP_3]_i$. The probable cause of the elevated basal $[Ca^{2+}]_i$ is continuous Ca^{2+} entry, because Ca^{2+} oscillations are dependent on external $[Ca^{2+}]$ in their frequency and are abolished in Ca^{2+}-free medium (*18*). Sperm may cause both persistent production of IP_3 and an increase in Ca^{2+} permeability of the plasma membrane to maintain Ca^{2+} oscillations.

REFERENCES AND NOTES

1. L. F. Jaffe, in *Biology of Fertilization*, C. B. Metz and A. Monroy, Eds. (Academic Press, New York, 1985), pp. 127–165; *Proc. Natl. Acad. Sci. U.S.A.* **88**, 9883 (1991).
2. M. Whitaker and R. Patel, *Development* **108**, 525 (1990).
3. S. Miyazaki *et al.*, *Dev. Biol.* **118**, 259 (1986). Mature hamster eggs were obtained from oviducts of superovulated female golden hamsters and freed from the surrounding cumulus cells and zona pellucida with hyaluronidase and trypsin. Eggs were bathed in modified Krebs-Ringer solution in a plastic dish mounted on an inverted microscope. Sperm were obtained from the cauda epididymides and were incubated for 5 hours.
4. M. J. Berridge and A. Galione, *FASEB J.* **2**, 3074 (1988); M. J. Berridge, *Cell Calcium* **12**, 63 (1991).
5. M. J. Berridge, P. H. Cobbold, K. S. R. Cuthbertson, *Philos. Trans. R. Soc. London Ser. B* **320**, 325 (1988); W. G. Wier and L. A. Blatter, *Cell Calcium* **12**, 241 (1991).
6. W. B. Busa, J. E. Ferguson, S. K. Joseph, J. R. Williamson, R. Nuccitelli, *J. Cell Biol.* **101**, 677 (1985).
7. S. Miyazaki, *ibid.* **106**, 345 (1988).
8. T. L. Rakow and S. S. Shen, *Proc. Natl. Acad. Sci. U.S.A.* **87**, 9285 (1990).
9. A. Galione, H. C. Lee, W. Busa, *Science* **253**, 1143 (1991)
10. S. Supattapone, P. F. Worley, J. M. Baraban, S. H. Snyder, *J. Biol. Chem.* **263**, 1530 (1988).
11. N. Maeda, M. Niinobe, K. Nakahira, K. Mikoshiba, *J. Neurochem.* **51**, 1724 (1988). For immunohistochemical staining of hamster eggs, oviducts containing mature eggs were removed, were fixed with Bouin's fixative and were embedded in paraffin. Sections (6 μm) were stained with an avidin-biotin complex. For immunoblot analysis, blotted proteins were reacted with each antibody and with peroxidase-conjugated goat antibody to rat or rabbit immunoglobulin G (IgG) (1:1000 dilution). Blots were incubated with enhanced chemiluminescence solution (Amersham, Buckinghamshire, England) and exposed on Kodak X-AR film.
12. H. Takeshima *et al.*, *Nature* **339**, 439 (1989).
13. T. Furuichi *et al.*, *ibid.* **342**, 32 (1989).

14. G. A. Mignery, C. L. Newton, B. T. Archer III, T. C. Südhof, *J. Biol. Chem.* **265**, 12679 (1990).
15. S. Nakade, N. Maeda, K. Mikoshiba, *Biochem. J.* **277**, 125 (1991).
16. F. J. Longo, *Anat. Res.* **179**, 27 (1974).
17. Injection pipettes of MAb contained MAb (0.3 to 3.6 mg/ml), 300 μM fura 2 (Molecular Probes Inc.), and 10 mM Hepes-KOH (pH 7.1). The volume injected was 10 to 25 pl, estimated from fura 2 fluorescence activated by 360-nm ultraviolet light (F_{360}). The intracellular concentration of MAb was calculated, assuming uniform distribution in the egg. IP_3 injection solution was 190 μM IP_3 (Boehringer Mannheim, Mannheim, Germany), 75 mM KCl, and 20 mM Hepes-KOH (pH 7.1). For Ca^{2+} imaging, 340-nm light from a xenon lamp and 340 ± 10 nm narrow band pass filter was applied throughout the Ca^{2+} measurement of 1 to 2 min. Images of F_{340} taken with a silicon intensifier target camera were accumulated during 0.5-s intervals every 2 s with an image processor (Hamamatsu Photonics, Argus-100, Hamamatsu, Japan). Images of F_{360} were recorded before and after F_{340} recording. Data were processed to calculate the ratio F_{340}/F_{360}, assuming linear degradation of F_{360}. The calibration curve of Ca^{2+} was obtained using Ca^{2+}-EDTAOH buffers.
18. Y. Igusa and S. Miyazaki, *J. Physiol. (London)* **340**, 611 (1983).
19. M. Iino, T. Kobayashi, M. Endo, *Biochem. Biophys. Res. Commun.* **152**, 417 (1988).
20. N. F. Zaidi *et al.*, *J. Biol. Chem.* **264**, 21737 (1989).
21. K. Swann and M. Whitaker, *J. Cell Biol.* **103**, 2333 (1986).
22. A. T. Harootunian, J. P. Y. Kao, S. Paranjape, R. Y. Tsien, *Science* **251**, 75 (1991).
23. M. Iino, *J. Gen. Physiol.* **95**, 1103 (1990).
24. I. Bezprozvanny, J. Watras, B. E. Ehrlich, *Nature* **351**, 751 (1991).
25. Y. Igusa and S. Miyazaki, *J. Physiol. (London)* **377**, 193 (1986).
26. P. H. Cobbold, A. Sanchez-Bueno, C. J. Dixson, *Cell Caicium* **12**, 87 (1991).
27. S. Miyazaki, *ibid.*, p. 205.
28. L. Missiaen, C. W. Taylor, M. J. Berridge, *Nature* **352**, 241 (1991).
29. Supported by Grants-in-Aid for General Scientific Research and for Scientific Research on Priority Areas (S.M.) and by a Grant for Specially Promoted Research (K.M.), from the Japan Ministry of Education, Science, and Culture. We thank G. Kuwajima for the antibody to the rabbit ryanodine receptor.

10 February 1992; accepted 8 May 1992

Syntaxin: A Synaptic Protein Implicated in Docking of Synaptic Vesicles at Presynaptic Active Zones

Mark K. Bennett, Nicole Calakos, Richard H. Scheller*

Synaptic vesicles store neurotransmitters that are released during calcium-regulated exocytosis. The specificity of neurotransmitter release requires the localization of both synaptic vesicles and calcium channels to the presynaptic active zone. Two 35-kilodalton proteins (p35 or syntaxins) were identified that interact with the synaptic vesicle protein p65 (synaptotagmin). The p35 proteins are expressed only in the nervous system, are 84 percent identical, include carboxyl-terminal membrane anchors, and are concentrated on the plasma membrane at synaptic sites. An antibody to p35 immunoprecipitated solubilized N-type calcium channels. The p35 proteins may function in docking synaptic vesicles near calcium channels at presynaptic active zones.

Chemical neurotransmitters are stored within the nerve terminal in synaptic vesicles that are often found associated with cytoskeletal components or the presynaptic plasma membrane (*1, 2*). Upon nerve stimulation, activation of voltage-gated Ca^{2+} channels in the nerve terminal plasma membrane results in an influx of Ca^{2+}. The increase in cytosolic Ca^{2+} concentration triggers the fusion of a portion of the synaptic vesicle population with the presynaptic plasma membrane, resulting in neurotransmitter release. The docking and subsequent fusion of synaptic vesicles with the presynaptic plasma membrane occur at a restricted, morphologically distinct domain known as the active zone (*2*). Because membrane fusion is initiated within 200 μs of the influx of Ca^{2+} (*3*), the cellular machinery mediating fusion is likely to be preassembled at sites of neurotransmitter release. The process of synaptic vesicle docking with the presynaptic membrane may represent the assembly of a prefusion complex that is likely to include components of each membrane. Three synaptic vesicle membrane proteins, p65 [synaptotagmin (*4–6*)], synaptophysin (*7, 8*), and synapsin I (*9*), exhibit properties suggestive of a role in synaptic vesicle docking or fusion.

We have focused on the biochemical characterization of p65, including the identification of proteins with which it interacts (*10*). p65 is a transmembrane protein with two repeats in the cytoplasmic domain homologous to the C2 regulatory domain of protein kinase C (*5*), a domain that may be important for interactions with the plasma membrane (*11*). To identify proteins that interact with p65, we solubilized a synaptic vesicle–enriched fraction from rat brain with different detergents and subjected it to immunoprecipitation with a monoclonal antibody to p65 (anti-p65) (*4*). The crude vesicle fraction used for these studies (*10, 12*) contains, in addition to synaptic vesicles, cytoskeletal and plasma membrane components that might interact with p65. Anti-p65 coprecipitated several synaptic vesicle proteins (*10*) and a set of 35-kD proteins (p35) (Fig. 1A). Anti-p65 also precipitated a protein kinase that phosphorylated both p65 and p35 in vitro (Fig. 1B). The protein kinase responsible for this phosphorylation is casein kinase II (*13*).

An oligonucleotide probe, based on an amino acid sequence obtained from the p35 proteins, was used to isolate seven cDNA clones from a rat brain cDNA library (*14*). On the basis of restriction enzyme mapping and nucleotide sequencing, these clones were divided into two classes, p35A and p35B (*15*). The predicted protein sequences encoded by the two classes of cDNA clones are 84% identical (Fig. 2). The sequence obtained by direct microsequencing of the p35 proteins was identical to that of p35A. No similarity with any protein sequence in the SWISS-PROT database was observed. Both p35A and p35B are highly charged (~38% charged amino acids) with an overall acidic isoelectric point (pI) (~5.1). However, the COOH-terminal 23 (p35A) or 24 (p35B) amino acids are very hydrophobic [average Kyte-Doolittle hydropathy scores (*16*) of 2.67 and 2.47, respectively], suggesting that this domain might serve as a membrane anchor. Because the p35 proteins lack an NH_2-terminal signal sequence, they may be membrane-anchored proteins with their NH_2-termini on the cytoplasmic side of the bilayer. This orientation would be similar to that of the synaptic vesicle protein VAMP (*17*). Northern (RNA) blot analysis (*13*) revealed that the p35A and p35B cDNA clones hybridized to 2.2- and 4.4-kb nervous system–specific transcripts, respectively.

The coimmunoprecipitation of p35 with p65 (Fig. 1A) suggested that these two proteins might interact directly. To investigate this possibility, we expressed full-length p35A and the cytoplasmic domain of p65 (p65-IIs) in bacteria (*18*) and mixed the two purified proteins in vitro. The mixture was immunoprecipitated with anti-p65 and analyzed by SDS–polyacrylamide gel electrophoresis (PAGE). Anti-p65 coprecipitated p65-IIs and p35A but not bovine serum albumin (BSA) included in the incubation as a nonspecific blocking agent (Fig. 3). A similar result was obtained with p35B (*13*). In the absence of p65-IIs, no p35A was immunoprecipitated. These results indicate that p65 and p35 interact directly.

To further characterize the biochemical

Howard Hughes Medical Institute, Department of Molecular and Cellular Physiology, Beckman Center for Molecular and Genetic Medicine, Stanford University Medical Center, Stanford, CA 94305.

*To whom correspondence should be addressed.